Universal ion exchange method for flowerlike metal telluride (PbTe, CdTe, Sb_2Te_3, Bi_2Te_3, and Cu_7Te_4) microstructures by using β-$ZnTe(en)_{0.5}$ as templates

Weiwei Xu[1,2], Guimin Tian[1], Xiaohua Ma[3], Hui Li[1], Jinzhong Niu[1] ✉

[1]*College of Science, Henan Institute of Engineering, Zhengzhou, 451191, People's Republic of China*
[2]*Key Laboratory for Special Functional Materials of Ministry of Education, Henan University, Kaifeng, 475004, People's Republic of China*
[3]*Golden Leaf Production and Manufacturing Center, China Tobacco Henan Industrial Co., Ltd., Zhengzhou, 450000, People's Republic of China*
✉ *E-mail: njz@haue.edu.cn*

Published in Micro & Nano Letters; Received on 23rd May 2018; Revised on 9th September 2018; Accepted on 1st October 2018

A universal ion exchange template-assisted route is successfully developed for preparing various three-dimensional (3D) metal telluride flowerlike microstructures, including PbTe, CdTe, Bi_2Te_3, Sb_2Te_3, and Cu_7Te_4. The proposed synthesis method is simple and reproducible. Firstly, organic–inorganic hybrid β-$ZnTe(en)_{0.5}$ flowerlike microcrystals are prepared as the template, and then a corresponding metal salt (Pb, Cd, Bi, Sb, and Cu) is introduced to synthesise the corresponding metal telluride flowerlike microstructures. During this process, ethylenediamine molecules and Zn ions in the β-$ZnTe(en)_{0.5}$ flowerlike microcrystals simultaneously exchange with metal ions (Pb, Cd, Bi, Sb, and Cu) after the addition of metal precursors, and finally form flowerlike metal telluride microcrystals. This method may be further extended for other 3D metal telluride microstructures.

1. Introduction: Metal tellurides with defined size and shape have been studied vigorously using many methods due to their potential applications in a variety of areas [1–4]. Among the synthesis methods, a two-step Te templating method has attracted great attention because it is simple and environment friendly [5, 6]. Due to Te atoms are bound together through van der Waals interactions in a hexagonal lattice, one-dimensional structures are preferentially formed and this limits the preparation of three-dimensional (3D) structures [7–9]. However, research of 3D metal tellurides is a useful field due to their application in water treatment and thermoelectricity. Recently, many efforts have been made to study the synthesis of organic–inorganic hybrid $ZnQ(en)_{0.5}$ (Q = S, Se) microcrystals [10–12] and use them to obtain different 3D-structured ZnO [13], ZnS [13], and ZnSe [14–16] by thermal treatment. Also to our knowledge, there is still no reports on well-defined 3D metal telluride structures by using organic–inorganic hybrid $ZnTe(en)_{0.5}$ structures as templates.

Herein, we develop a simple and general template-directed route to fabricate metal telluride 3D microstructures by using organic–inorganic hybrid β-$ZnTe(en)_{0.5}$ flowerlike microcrystals as templates. The ethylenediamine (EN) molecules and Zn ions in β-$ZnTe(en)_{0.5}$ structures are exchanged by the metal ions (Pb, Cd, Bi, Sb, and Cu) during the reaction, and five types of metal telluride flowerlike microcrystals (PbTe, CdTe, Bi_2Te_3, Sb_2Te_3, and Cu_7Te_4) have been successfully synthesised. The synthesis mechanism is also discussed based on the experimental results.

2. Experimental section: All the chemicals used were of analytical grade and without further purification. In a typical synthesis of flowerlike metal telluride, 0.041 g of CH_3COONa, 0.056 g of Na_2TeO_3, 0.200 g of polyvinylpyrrolidone (PVP) (molecular weight 30,000), 0.880 g of $Zn(CH_3COO)_2$, 2.0 mL of EN, and 10.0 mL of ethylene glycol (EG) were put into a 50 mL three-neck flask. After vigorous stirring for 60 min at 40°C, the temperature was raised to 175°C and maintained for 2 h under a 2 L/min flow rate of refluxing water. A corresponding metal salt ($Pb(ac)_2$ (0.25 mmol), $Sb(ac)_3$ (0.17 mmol), $BiCl_3$ (0.17 mmol), $Cd(ac)_2$ (0.25 mmol), and $Cu(ac)_2$ (0.25 mmol)) was added into the flask, respectively. During this process, the colour of the reaction solution immediately changed from grey to black. Also the reactions were lasted for another 1 h, PbTe, Sb_3Te_2, Bi_2Te_3, CdTe, and Cu_7Te_4 flowerlike microcrystals were formed, respectively. For purification, 50 mL of absolute ethanol was added and the byproducts were removed by centrifugation. Finally, the powder products were obtained after 8 h of drying at 65°C. The as-prepared products were characterised using a Bruker D8 advance X-ray powder diffractometer, an FEI Quana-250 electron microscope, a Thermo Fisher Nicolet 6700 Fourier infrared spectroscope, a Renishaw inVia Reflex Raman spectroscope, and Netzsch STA449 F3 thermal analysis.

3. Results and discussion: Fig. 1 displays a panoramic scanning electron microscope (SEM) image of various as-synthesised products. The flowerlike β-$ZnTe(en)_{0.5}$ and metal telluride microcrystals are shown in Fig. 1*a–f*, respectively. The petals of the synthesised flowerlike structures have a uniform sheet morphology with a mean lateral size of several micrometres. It should be noted that the dimensions and thickness of Bi_2Te_3, Cu_7Te_4, and PbTe are basically remained after the addition of metal ions (Pb, Bi, and Cu) compared with the β-$ZnTe(en)_{0.5}$ template. While, the petals of CdTe (Fig. 1*c*) and Sb_2Te_3 (Fig. 1*e*) flowerlike structures are different from those of the β-$ZnTe(en)_{0.5}$ template. We speculate that the relative small ion radius of Cd and Sb caused a crush and reconstruction process, and CdTe and Sb_2Te_3 still bear a flowerlike morphology. Atomic molar ratios of X:Te (X = Zn, Pb, Cd, Bi, Sb and Cu) is nearly 1:1, 1:1, 1:1, 2:3, 2:3, and 7:4 as shown in the insets of Fig. 1.

The crystal phases of metal telluride microcrystals are characterised and are shown in Fig. 2. The β-$ZnTe(en)_{0.5}$ pattern shows an orthorhombic structure with the space group of *Pnnm* (58), which is refined by Rietveld analysis in Fig. 2*a*. The cell lattice parameters are calculated to be $a = 5.672$, $b = 4.350$, and $c = 17.173$, which is in good agreement with previous literatures [17, 18]. The strong and sharp diffraction peaks suggest good crystallinity and large particle sizes of β-$ZnTe(en)_{0.5}$. After the addition of metal precursors (Pb, Cd, Bi, Sb, Cu), the products change from organic–inorganic hybrid β-$ZnTe(en)_{0.5}$ microcrystals to metal telluride microcrystals. All the patterns of metal telluride crystals,

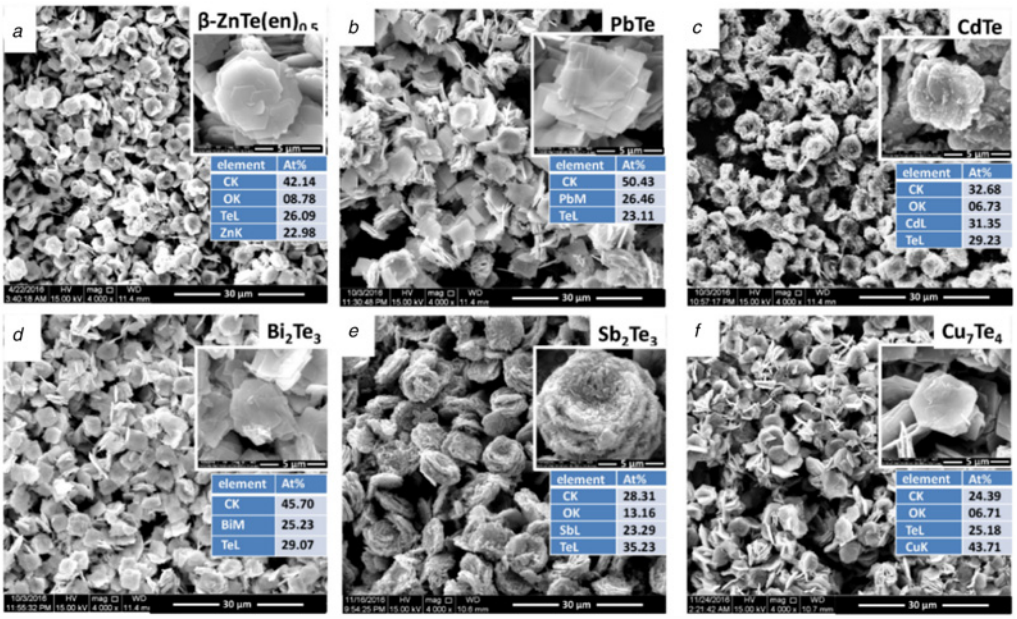

Fig. 1 *SEM images of*
a β-ZnTe(en)$_{0.5}$
b PbTe
c CdTe
d Bi_2Te_3
e Sb_2Te_3, and
f Cu_7Te_4 flowerlike microstructures. The inset table is respective EDX result of (a) β-ZnTe(en)$_{0.5}$, (b) PbTe, (c) CdTe, (d) Bi_2Te_3, (e) Sb_2Te_3, and (f) Cu_7Te_4 microcrystals

PbTe (cubic, JCPDS Card No. 38-1435, Fig. 2*b*), CdTe (cubic, JCPDS Card No. 15-0770, Fig. 2*c*), Bi_2Te_3 (hexagonal, JCPDS Card No. 08-0027, Fig. 2*d*), Sb_2Te_3 (hexagonal, JCPDS Card No. 15-0874, Fig. 2*e*), and Cu_7Te_4 (hexagonal, JCPDS Card No. 45-1287, Fig. 2*f*) are in agreement with the corresponding standard diffraction patterns. These results are consistent with the energy-dispersive X-ray spectroscopy (EDX) results shown in Fig. 1.

Fourier transform infrared (FTIR) spectra are characterised and shown in Fig. 3*a* to prove the surface ligands of products. For β-ZnTe(en)$_{0.5}$, the bands at 3117 and 3206 cm^{-1} are attributed to the NH_2 asymmetric and symmetric stretching vibrations, which shift towards lower frequency compared with pure EN molecules, suggests that EN molecules have been intercalated into the β-ZnTe(en)$_{0.5}$ template [9]. The bands at 3437 and 1638 cm^{-1}, correspond to the O–H stretching vibrations, could be attributed to the absorption of EG and H_2O in the sample. After the addition of metal precursors (Pb, Cd, Bi, Sb, and Cu), the disappearance of NH_2 vibrations (3117 and 3206 cm^{-1}) in the final products proves that metal ions (Pb, Cd, Bi, Sb, and Cu) have exchanged with EN molecules and Zn ions simultaneously and finally form metal telluride crystals. Other absorption bands at 2921, 2854, 1635, 1404, and 1296 cm^{-1} are in accordance with pure PVP (Fig. 3*b*), which proves that PVP acts as the surface ligands for all metal telluride products.

To further ascertain the ligands of flowerlike microcrystals, thermogravimetric-differential scanning calorimetry (TG-DSC) results are shown in Fig. 4. For β-ZnTe(en)$_{0.5}$, the 10% weight loss with exothermic reaction locating at 298°C is attributed to the decomposition of intercalated EN molecules in β-ZnTe(en)$_{0.5}$ (Fig. 4*a*). After the addition of metal ions (Pb, Cd, Bi, Sb, and Cu), the disappearance of exothermic curve at 298°C also indicates that EN molecules in β-ZnTe(en)$_{0.5}$ have been exchanged by metal ions (Pb, Cd, Bi, Sb, and Cu).

Based on earlier experimental results and analysis, the whole morphology evolution process of products is proposed. In the initial stage, Te ions react with Zn ions and EN molecules to form flowerlike β-ZnTe(en)$_{0.5}$ crystals, in which every adjacent two monolayers of zinc-blende ZnTe are inter-connected by EN molecules which are bonded to Zn atoms [18]. Similar to previous reports [12, 19], after thermal decomposition of ZnTe(en)$_{0.5}$, the disappearance of EN molecules causes the formation of pore structures. In our experiments, different ion radii of Pb^{2+} (0.120 nm), Cd^{2+} (0.097 nm), Bi^{3+} (0.108 nm), Sb^{3+} (0.092 nm), and Cu^{1+} (0.096 nm) will result different structures by the exchange for Zn ions and EN molecules. From the SEM results in Fig. 1, we found that the petals of PbTe (cubic), Bi_2Te_3 (hexagonal), and Cu_7Te_4 (hexagonal) are remained compared with β-ZnTe(en)$_{0.5}$. While, for CdTe (cubic) and Sb_2Te_3 (hexagonal) microcrystals, the petals crushed and reconstructed though the flowerlike structures are remained. We speculate that the ion radius determined the process. The relative larger ion radii of Pb^{2+} (0.120 nm) and Bi^{3+} (0.108 nm) seem suitable to fill the pores in the β-ZnTe(en)$_{0.5}$ templates. While, for CdTe (cubic) and Sb_2Te_3 (hexagonal) microcrystals, the smaller ion radii (Cd^{2+} of 0.97 nm and Sb^{3+} of 0.92 nm) means they are not large enough to fill the pores and the petals are reconstructed after exchange. Although Cu^{1+} (0.096 nm) and Sb^{3+} (0.092 nm) have similar cation radius, the higher molar ratio of Cu_7Te_4 (hexagonal) than that of Sb_2Te_3 (hexagonal) may be the main reason for remaining the petal structure and avoid crushing effectively. In addition, morphology of metal tellurides (PbTe, Bi_2Te_3, and Cu_7Te_4) has some changes when compared with β-ZnTe(en)$_{0.5}$ due to the different binding forces between the metal and Te ions. As depicted earlier, the reaction process can be formulated as follows:

$$2Zn^{2+} + 2Te^{2-} + EN \rightarrow 2ZnTe(en)_{0.5} \quad (1)$$

$$2Pb^{2+} + 2ZnTe(en)_{0.5} \rightarrow 2PbTe + 2Zn^{2+} + EN \quad (2)$$

The Raman scattering spectral analyses performed on flowerlike structures are depicted in Fig. 5. The sharp Raman lines show the presence of β-ZnTe(en)$_{0.5}$ with characteristic bands at 120.1,

doi: 10.1049/mnl.2018.5209

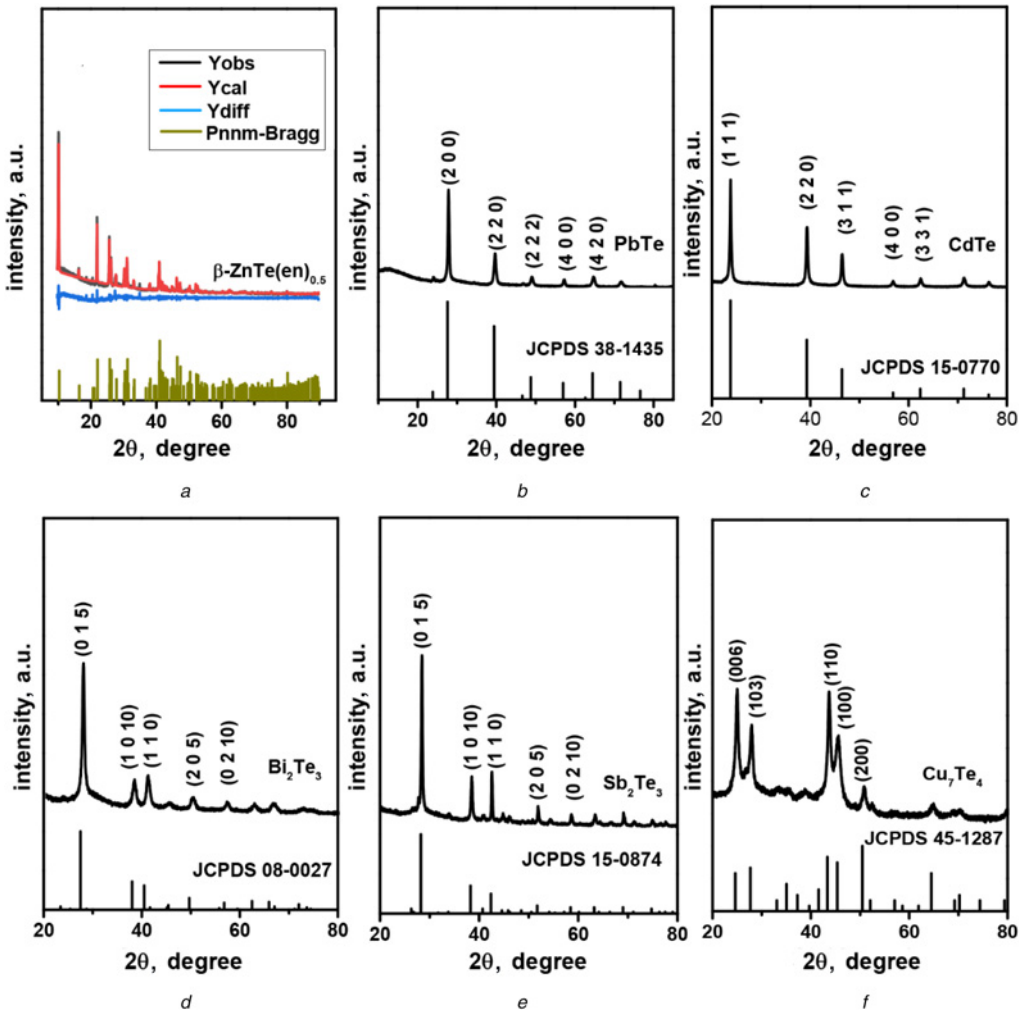

Fig. 2 *XRD patterns of*
a the Rietveld analysis of the XRD pattern of β-ZnTe(en)$_{0.5}$ for *Pnnm*. The $R_{exp} = 4.2$, $R_{wp} = 9.29$, and $R_p = 7.53$; the black solid line, red dot line, and blue solid line represent the observed, calculated, and difference profiles, respectively
b PbTe
c CdTe
d Bi_2Te_3
e Sb_2Te_3, and
f Cu_7Te_4 microcrystals. The claybank bars indicate the positions of corresponding Bragg peaks for (a) β-ZnTe(en)$_{0.5}$, (b) PbTe, (c) CdTe, (d) Bi_2Te_3, (e) Sb_2Te_3, and (f) Cu_7Te_4

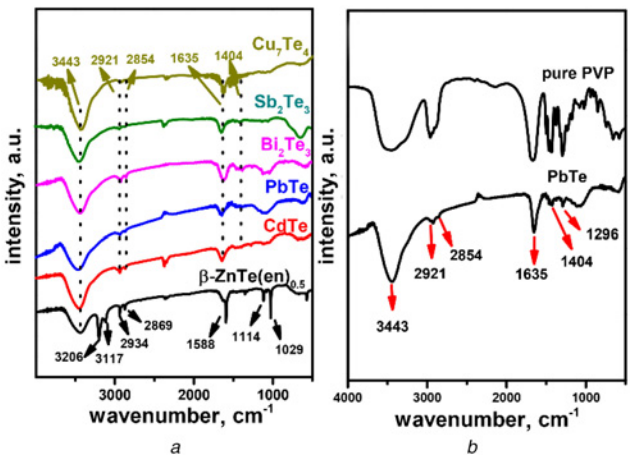

Fig. 3 *FTIR spectra of*
a As-synthesised flowerlike microstructures and
b pure PVP

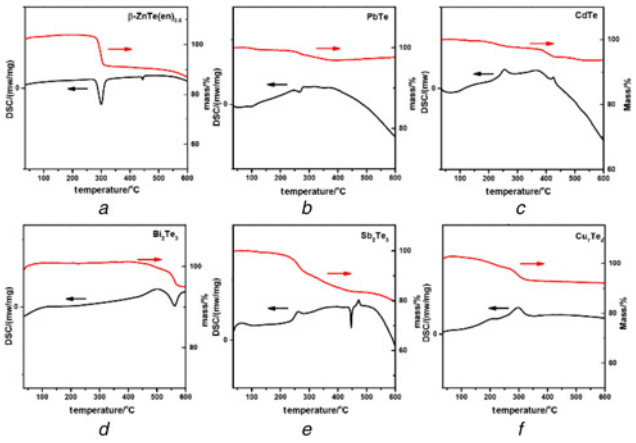

Fig. 4 *TG-DSC curves of the as-synthesised*
a β-ZnTe(en)$_{0.5}$
b PbTe
c CdTe
d Bi_2Te_3
e Sb_2Te_3, and
f Cu_7Te_4 flowerlike microstructures

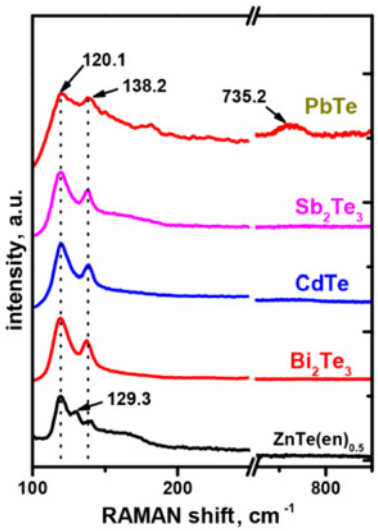

Fig. 5 *Raman spectra of the as-synthesised flowerlike microstructures*

129.2, and 138.2 cm^{-1}, which have also been observed by the Huang group [20]. After the addition of metal precursors (Pb, Cd, Bi, Sb, and Cu), there are two Raman peaks at 120.1 and 138.2 cm^{-1} for Bi_2Te_3, CdTe, Sb_2Te_3, and PbTe samples, which are similar to β-$ZnTe(en)_{0.5}$ and are attributed to A_1 (Te), E (Te), or TO (TeO_2), respectively. These results are close to previous reports on Bi_2Te_3 [20, 21], CdTe [22], Sb_2Te_3 [23], and PdTe [24] structures, respectively. The peaks at 732.5 cm^{-1} for the PbTe sample are attributed to the higher-harmonic multiphonon process [24]. The disappearance of the 129.2 cm^{-1} peak means the β-$ZnTe(en)_{0.5}$ have changed to metal tellurides.

4. Conclusion: In this Letter, we report a convenient route to prepare a variety of flowerlike metal telluride 3D microcrystals by using β-$ZnTe(en)_{0.5}$ flowerlike structures as templates. The proposed synthesis method is simple and reproducible. The EN molecules and Zn ions in the β-$ZnTe(en)_{0.5}$ structure are exchanged by the metal ions (Pb, Cd, Bi, Sb, and Cu) during the reaction. This simple approach to fabricate flowerlike 3D metal telluride microstructures can be easily scaled-up and it shows the potential in thermoelectricity and photocatalysis areas.

5. Acknowledgments: This study was funded by the program for key scientific research projects in colleges and universities of Henan province (grant no. 16A140026), doctor fund of Henan Institute of Engineering (grant no. D2014005), support program for young backbone teachers of colleges and universities in Henan province (grant no. 2015GGJS-032), and Henan Province University Scientific and Technological Innovation Team (grant no. 18IRTSTHN005).

6 References

[1] Yang J., Gao Y., Kim J.W., *ET AL.*: 'Self-reorganization of CdTe nanoparticles into two-dimensional Bi_2Te_3/CdTe nanosheets and their thermoelectrical properties', *Phys. Chem. Chem. Phys.*, 2010, **12**, (38), pp. 11900–11904

[2] Zhou C., Dun C., Wang Q., *ET AL.*: 'Nanowires as building blocks to fabricate flexible thermoelectric fabric: the case of copper telluride nanowires', *ACS Appl. Mater. Interfaces*, 2015, **7**, (38), pp. 21015–21020

[3] Major J.D., Treharne R.E., Phillips L.J., *ET AL.*: 'A low-cost non-toxic post-growth activation step for CdTe solar cells', *Nature*, 2014, **511**, (7509), pp. 334–337

[4] Shen H., Zheng Y., Wang H., *ET AL.*: 'Highly efficient near-infrared light-emitting diodes by using type-II CdTe/CdSe core/shell quantum dots as a phosphor', *Nanotechnology*, 2013, **24**, (47), pp. 475603–475603

[5] Fan H., Zhang Y., Zhang M., *ET AL.*: 'Glucose-assisted synthesis of cote nanotubes in situ templated by Te nanorods', *Cryst. Growth Des.*, 2008, **8**, (8), pp. 2838–2841

[6] Simpson R.E., Fons P., Kolobov A.V., *ET AL.*: 'Enhanced crystallization of GeTe from an Sb_2Te_3 template', *Appl. Phys. Lett.*, 2012, **100**, (2), p. 021911

[7] Dong G.H., Zhu Y.J., Cheng G.F., *ET AL.*: '$Cu_{(2-X)}Te$ nanowires synthesized by a microwave-assisted solvothermal method using a self-sacrificial template and their electrical conductivity', *Mater. Lett.*, 2012, **76**, (1), pp. 69–72

[8] Narayanan R., Sarkar D., Som A., *ET AL.*: 'Anisotropic molecular at 1 V from tellurium nanowires (Te NWs)', *Anal. Chem.*, 2015, **87**, (21), pp. 10792–10798

[9] Wu X., Wang Y., Zhou S., *ET AL.*: 'Morphology control, crystal growth, and growth mechanism of hierarchical tellurium (Te) microstructures', *Cryst. Growth Des.*, 2012, **13**, (1), pp. 136–142

[10] Huang X., Li J.: 'From single to multiple atomic layers: a unique approach to the systematic tuning of structures and properties of inorganic–organic hybrid nanostructured semiconductors', *J. Am. Chem. Soc.*, 2007, **129**, (11), pp. 3157–3162

[11] Huang X., Roushan M., Emge T.J., *ET AL.*: 'Flexible hybrid semiconductors with low thermal conductivity: the role of organic diamines', *Angew. Chem. Int. Ed.*, 2009, **48**, (42), pp. 7871–7874

[12] Li X., Wei B., Wang J., *ET AL.*: 'Synthesis and comparison of the photocatalytic activities of $ZnSe(En)_{0.5}$, ZnSe and ZnO nanosheets', *J. Alloys Compd.*, 2016, **689**, pp. 287–295

[13] Jang J.S., Yu C.J., Sun H.C., *ET AL.*: 'Topotactic synthesis of mesoporous ZnS and ZnO nanoplates and their photocatalytic activity', *J. Catal.*, 2008, **254**, (1), pp. 144–155

[14] Yan Z., Hu C., Feng B., *ET AL.*: 'Synthesis and photocatalytic property of ZnSe flowerlike hierarchical structure', *Appl. Surf. Sci.*, 2011, **257**, (24), pp. 10679–10685

[15] Yang J., Wang G., Hao L., *ET AL.*: 'Solvothermal synthesis and characterization of ZnSe nanoplates', *J. Cryst. Growth*, 2008, **310**, (15), pp. 3645–3648

[16] Zhang L., Yang H., Xie X., *ET AL.*: 'Preparation and photocatalytic activity of hollow ZnSe microspheres via Ostwald ripening', *J. Alloys Compd.*, 2009, **473**, (1–2), pp. 65–70

[17] Huang X., Li J., Zhang Y., *ET AL.*: 'From 1D chain to 3D network: tuning hybrid II–VI nanostructures and their optical properties', *J. Am. Chem. Soc.*, 2003, **125**, (23), pp. 7049–7055

[18] Moon C.Y., Dalpian G.M., Zhang Y., *ET AL.*: 'Study of phase selectivity of organic–inorganic hybrid semiconductors', *Chem. Mater.*, 2006, **18**, (12), pp. 2805–2809

[19] Nasi L., Calestani D., Besagni T., *ET AL.*: 'ZnS and ZnO nanosheets from $ZnS(En)_{0.5}$ precursor: nanoscale structure and photocatalytic properties', *J. Phys. Chem. C*, 2012, **116**, (12), pp. 6960–6965

[20] Park D., Park S., Jeong K., *ET AL.*: 'Thermal and electrical conduction of single-crystal Bi_2Te_3 nanostructures grown using a one step process', *Sci. Rep. (UK)*, 2016, **6**, p. 19132

[21] Chen L., Zhao Q., Ruan X.: 'Facile synthesis of ultra-small Bi_2Te_3 nanoparticles, nanorods and nanoplates and their morphology-dependent Raman spectroscopy', *Mater. Lett.*, 2012, **82**, (9), pp. 112–115

[22] Ma L., Wei Z., Zhang F., *ET AL.*: 'Synthesis and characterization of high-ordered CdTe nanorods', *Superlattices Microstruct.*, 2015, **88**, pp. 536–540

[23] Secor J., Harris M.A., Zhao L., *ET AL.*: 'Phonon renormalization and Raman spectral evolution through amorphous to crystalline transitions in Sb_2Te_3 thin films', *Appl. Phys. Lett.*, 2014, **104**, (22), p. 221908

[24] Bali A., Kim I.H., Rogl P., *ET AL.*: 'Thermoelectric properties of two-phase PbTe with indium inclusions', *J. Electron. Mater.*, 2014, **43**, (6), pp. 1630–1638

doi: 10.1049/mnl.2018.5209